An engineering development of a novel hexrotor vehicle for 3D applications

D. Langkamp, G. Roberts, A. Scillitoe, I. Lunnon, A. Llopis-Pascual, J. Zamecnik, S. Proctor, M. Rodriguez-Frias, M. Turner, A. Lanzon and W. Crowther

University of Manchester, George Begg Building, Sackville Street, M13 9PL,UK

Abstract

This paper is about the development of a novel type of non coplanar hex rotor with the ability to decouple translational and attitude dynamics. The proposed design features six variable pitch rotors arranged in three different rotor planes in order to point the thrust and torque vectors independently of body attitude. It is envisaged that this design could be beneficial for operations in confined spaces where the requirements for translational control authority design outweigh the reduced hover efficiency compared to coplanar multi rotors, such as quad rotors.

The rotor arrangement leads to design and modeling challenges which are very different from those of conventional planar multi rotor vehicles. The key engineering challenge lies in the requirement to generate sufficient thrust for weight support with two rotors alone. This paper shows how this challenge was overcome by the use of high thrust/weight electric variable pitch units and a low airframe mass fraction. The design of avionics and indoor positioning solutions is discussed and the control strategies are outlined. The development and wind tunnel validation of a simulation model is discussed and operational modes are presented which satisfy the key constraints, linearise the thrust response and optimise hover efficiency.

The feasibility of the concept was demonstrated through the flight testing of fixed-pitch design in 2009 and a flight demonstration of the variable pitch design is planned for IMAV 2011.

1 INTRODUCTION

This paper presents the engineering design of a novel non planar hexrotor vehicle with the capability to decouple translational and attitude dynamics [6]. This is achieved by arranging the six rotors on three separate planes such that the thrust and torque vectors can be pointed independently.

The "Tumbleweed" hexrotor concept was originally developed as a rotary wing vehicle for operation in the interface zone between urban structures and the airspace adjacent to these structures. The capability to vector thrust independent of body attitude enables manoeuvring in confined spaces and provides the ability to land and take off at arbitrary body attitudes. These performance improvements come at the cost of reduced hover efficiency and increased mass compared to planar rotorcraft solutions and hence there has to be a suitable trade off between improved manoeuvrability and reduced payload, range and endurance.

A prototype vehicle with fixed pitch propellers and flown in a similar manner to a conventional planar rotary wing vehicle was flown in 2009. The present hexrotor work is distinct to previous published work on multi-rotor UAVs, e.g. [1-3], which considers only coplanar rotor systems and is predominantly based on fixed-pitch rotors. A similar operating principle to the hexrotor was introduced by Salazar [4] who used a fixed-pitch quadrotor with four thrusters to provide side-forces. Although this concept also provides means to decouple attitude and translational dynamics it requires at least 8 rotors and can only be used over a limited range of body attitudes.

Figure 1: Test flight of a fixed-pitch hexrotor in November 2009

Our previous work on the hexrotor [5, 6] introduced the concept, described appropriate control strategies and demonstrated practical feasibility in near hover conditions. This paper goes further by presenting the engineering design and modelling of a variable pitch hexrotor system with increased control authority compared to the previous fixed-pitch design. It is shown how such a vehicle can be designed using off-the-shelf systems, open source electronics and rapid prototyping solutions. Furthermore, a collective-pitch/rpm envelope is presented that satisfies the design constraints whilst optimising the combined electric and aerodynamic efficiency for typical operating conditions. The feasibility of the proposed design is demonstrated through simulations and wind tunnel testing.

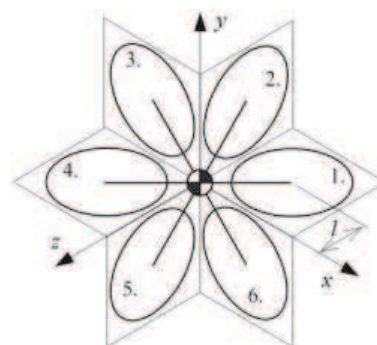## 2 VEHICLE DESIGN SPECIFICATION

2.1 Systems concept

Figure 2: Orthogonal face-centred hexrotor configuration and body coordinate system

The way in which the six rotors are arranged into three rotor planes is a trade-off between hover efficiency and torque control authority (the interested reader is referred to [6] for details). However, the highest authority and most energy efficient thrust vectoring occur when the force characteristic axes are orthogonal such as in the configuration shown in Figure 2. This is the most energy efficient configuration for a hexrotor with decoupled translational and attitude dynamics, because is has the largest rotor disk area projected on the horizontal plane and hence the induced power requirement. The default orientation of the vehicle is such that equal weight support is provided by each rotor and the earth-z axes aligns with the resultant of [-1,-1,-1] in body coordinates.

In order to provide full authority (4pi steradians) of thrust and torque vectoring on a hover capable hexrotor configuration two key design constraints need to be met: a) the direction of thrust must be reversible and b) two rotors must be able to provide sufficient thrust to lift the vehicle. The latter proved to be the hardest constraint since it resulted in increased pressure on component performance and mass targets compared to those for typical planar multi-rotor designs. The approach taken was to design the propulsion group for maximum thrust/weight ratio at the expense of pure hover efficiency. There was also aggressive programme to minimise structural mass.

The system sizing was based on an electrically powered vehicle in the 1kg class suitable for indoor operations. A CAD illustration of the prototype is shown in Figure 3.
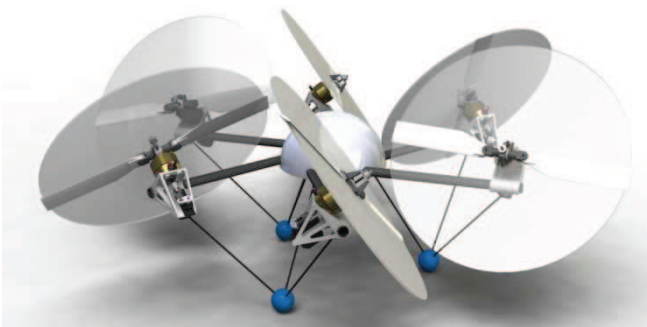

Figure 3: CAD rendering of prototype vehicle showing the orthogonal rotor planes. Rotor diameter 0.25m
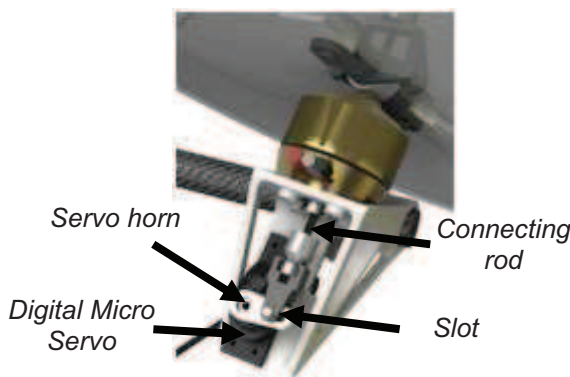
2.2 Electric Variable Pitch Propulsion

Figure 4: EVP unit driven by a digital servo

Electric Variable Pitch Propulsion (EVP) systems are commonly used for 3D aerobatic model aircraft. EVP systems typically consist of a DC electric motor and a hollow shaft. A connecting rod passes through the hollow shaft and is secured to a pitch horn so that the collective pitch of the symmetrical blades can be varied by pushing/pulling the connecting rod. The pitch actuation mechanism had to provide rapid pitch changes at a fine pitch resolution which is typically not required for fixed-wing aerobatic aircraft.

A pitch control mechanism consisting of a digital micro servo and slotted servo horn was chosen (Figure 4). The servo horn is slotted to prevent the transfer of lateral forces to the pin hence reducing the bending moment experienced by the connecting rod. A lower bending moment on the connecting rod means less friction between it and the hollow motor shaft, which leads to greater pitch control authority at high rotational speeds. The mechanism allows for a trade-off between pitch resolution and pitch response speed; a large servo moment arm gives a rapid pitch response but poor pitch resolution, while a small moment arm leads to the opposite. The mechanism also provides for an extremely compact geometry and easy to set-up design. The servo position was calibrated against the blade pitch under static conditions and the repeatability was tested using thrust and motor loading data.

Based on preliminary vehicle sizing and propulsion system mass fractions, to achieve flight a thrust/weight ratio of approximately 6.6 is required from each EVP system. Based on the EVP unit mass breakdown as shown in Table 1 this equates to a thrust of 6.3 N per EVP unit. Other important requirements are an identical performance when running in both clockwise and anti-clockwise rotary directions; a symmetrical thrust verses pitch curve with a large linear region to simplify control; small dimensions; and a mechanically simple design. The propulsion system thrust/weight ratio is at the limit of commercially available EVP systems, hence achieving the required maximum thrust is a key challenge. Finally, due to the lack of a significant incoming airflow heating issues were expected.

Component	Weight (g)
Brushless motor	45
Servo	8
EVP System, Hub and blades	19
25A ESC	17
Power connectors	7.5
Total =	96.5

Table 1: Mass breakdown of an EVP unit based on the AXI 2208/20

Table 1 shows the mass breakdown of the EVP unit. Whilst most components are comparable in mass to similar sized fixed-pitch systems, there is a mass penalty of about 10-20% due to the need for an additional actuator for blade pitch control and the increased mass of the rotor hub.

2.3 Structural design

The main constraint on the airframe structural design was to minimise mass in order to enable hovering on two rotors. The preliminary target mass for the airframe was defined as

10% (~100g) of the total takeoff mass. Further requirements were simplified construction and repair following damage.

The rotor arms are off the shelf carbon fibre tubing, cut to length using hand tools. The sizing of the carbon fibre tubing was based on static and dynamic finite element analysis and was checked experimentally, chosen for minimal bending deformation and a natural frequency above the motor rpm range.

All other components are manufactured from ABS plastic using an in-house low cost additive 3D printer (stereo-lithography). Using this technology complex parts, such as motor mounts ensuring the correct alignment of the rotor orientation, can be produced. This same method can be used to accurately align the rotors in the three rotor planes by printing components for an assembly jig. The strength to weight ratio of these components is sufficient for them to be evaluated on the vehicle. A strict mass reduction plan was followed using commercial finite element software to ensure the components would not fail under maximum load. An example for this the mass-minimisation strategy is the optimised centre-piece shown in Figure 5. The use of the in-house printer means design iterations are in the order of minutes or hours, and replacement components for repairs can be reproduced quickly.
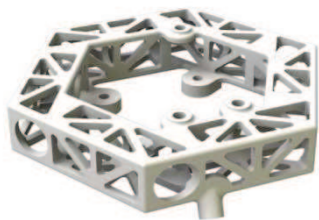

Figure 5: CAD model of the hexrotor centre piece showing the mass minimisation efforts

The vehicle's landing gear consists of three tripods consisting of carbon fibre struts and a foam ball. The landing gear struts were sized to ensure sufficient rotor ground clearance at a landing up to a 45° pitch or roll attitude. The chosen arrangement provided an easily replaceable landing gear as well as a desired structural failure point, minimising damage to the vehicle, with minimal mass penalty.

2.4 Indoor positioning solutions

Closed loop position and attitude control requires absolute measurement of position and/or attitude. In the absence of GPS for indoor testing, two relatively low cost positioning systems have been considered. The first is based on the use of time of flight measurements from ultrasonic beacons and the second is an optical based system using augmented reality markers.

For the ultrasonic solution a master unit equipped with multiple receivers is mounted on the vehicle. Each of the external slave units (currently 3) is commanded via the radio modem to emit a pulse. The master unit then calculates time of flight and therefore distance to slave unit for each of the vehicle receivers. This provides both position and attitude to the flight controller via the SPI bus.

In the visual system, Augmented Reality (AR) markers are used as an absolute metric for location detection. This approach consists of the use of a standard low cost camera and custom software developed to identify and localize specially designed AR markers.

The camera is initially calibrated offline using an existing MATLAB toolbox [7]. Algorithms from this toolbox extract the camera's intrinsic parameters including; focal length, principle point, skew, distortion and pixel error. These parameters are used for software configuration allowing the camera to be used as a projective sensor. In order to detect the markers a modified version of [9] is used to robustly detect edge pixels and then collect them to create line structures using RANSAC. A coarse grid system is used to obtain real-time performance.

The AR markers were specially designed to be identified within this UAV environment and operate in colour space rather than gray scale as is more usual. Once the markers have been detected the corner points were used to create a series of points that, when combined with the camera properties result in the position of the camera relative to the markers. The software was developed in C++, using OpenCV [8] for platform independence and for common image processing functions.

The main issue with the current AR approach is that this system only works with a single camera, however to get adequate coverage of a test area multiple cameras will be needed. There are also issues to be resolved with errors due to the non-uniform lighting of the AR markers.

Marker Size	1.5m	2m	2.5m	3m
8cm	100%	80%	20%	0%
10cm	100%	100%	50%	20%
12cm	100%	100%	100%	100%

Table 2: Optical positioning system performance against distance of camera from vehicle (percent of successfully recognized markers)

Although this method is currently limited by the effective detection range, with the right control of the camera the use of AR markers can be used as part of a complete solution for UAV localization within a controlled test area.

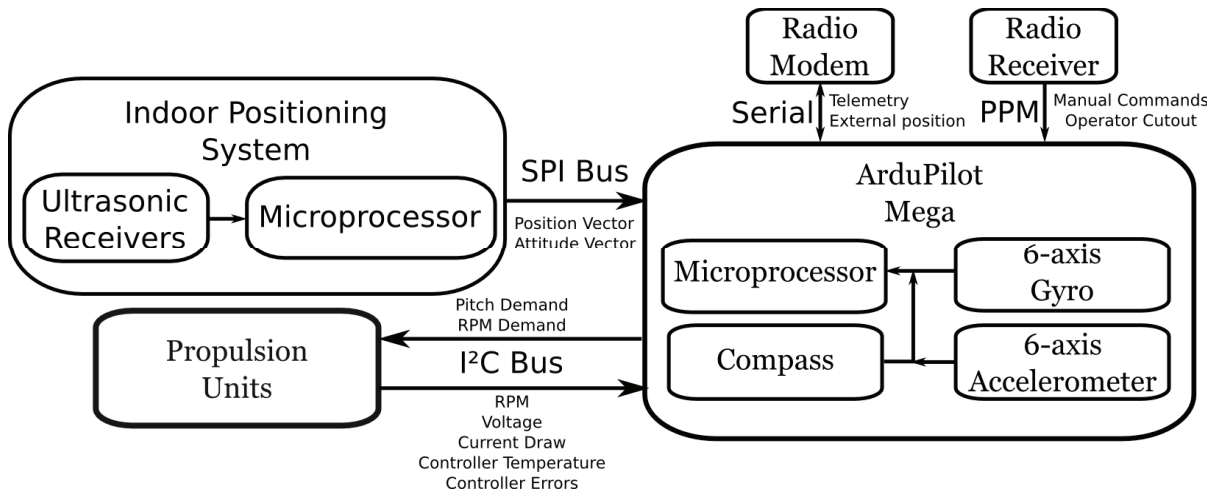Figure 6: Example of the AR markers

Figure 7: Avionics system block diagram highlighting major components

2.5 Avionics solution

In order to reduce costs and reduce development time, the onboard electronics package is based on the use of open-source hardware and open source software.

Stabilization and guidance is controlled using an open-source autopilot unit called ArduPilot Mega [10] The unit comprises of:

- ATMega 1280 microprocessor
- 3-axis gyros and 3 axis accelerometers
- Absolute pressure sensor
- On-board datalogging

The design is compatible with devices from the Arduino project [11], which focuses on simple to use devices for prototyping embedded applications. ArduPilot uses the same software ecosystem but with a form factor more suitable for micro-avionics use.

Control software is based upon code from both the ArduPilot and AeroQuad projects [11]; this reduces development time by providing proven libraries for common autopilot tasks to which the unique control algorithms required for this project are being implemented.

Digi XBee 2.4 Pro wireless modems provide bi-directional telemetry and manual control is via a standard Spektrum 2.4GHz 12 channel transmitter and a 2.4GHz DSM2 receiver to minimize interference issues. A decision was made to use BL-CTL V1.2 speed controllers from the Mikrokopter [12] project. These units provide open source access to controller algorithms, allow the flight controller to query each propulsion unit about current draw, rotational velocity and temperature and are also approximately 25-35% lighter than similar specification commercial speed controllers.

Power is supplied by a commercially available 3-cell lithium-polymer battery, and is distributed to all speed controllers and avionics via a common power bus.

3 CONTROL STRATEGIES

3.1 Bi-state control principle

Because of the novel actuation architecture of this vehicle standard quadrotor control algorithms are not suitable. Instead, the vehicle uses what is referred to as a bi-state control scheme: In the translational state the vehicle rotational axes are fixed relative to earth axis and the vehicle is commanded to translate in the Earth fixed x, y and z directions. In the rotational state, the vehicle position is fixed and control inputs are used to change the orientation of the vehicle. Control inputs may be rotations (or rates) about either the vehicle body axes or the earth fixed axes. Rotation and position are persisted across state changes allowing the operator to rotate the vehicle into the correct orientation before translating toward the region of interest (within the limits of actuator saturation).

3.2 Static mapping control strategy

To reduce the thrust time constant of the propulsion system the proposed mode of operation is to run the propulsion system at a constant base rotational speed and achieve control through variable-pitch alone.

Full state feedback control for the vehicle has previously been synthesised and presented in [6]. This section is included in order to outline some of the implementation issues encountered.

The decoupling of force and torque inherent in the design of the vehicle imply a decoupling between translation and attitude. Therefore, the vehicle effectively has two controllers, which independently calculate the required force and torque vectors for the vehicle. A mapping function then translates these vectors into a pitch command for each propulsion unit.

The controllers are implementation specific; example controllers derived using classical theory can be found in [6] and these controllers form the basis of the ones used on board the current vehicle. The mapping function however is of interest as it is specific only to the general vehicle configuration.

For a required force and torque response, assuming static conditions such as around hover, a requirement vector $[u_1 \quad u_2 \quad u_3 \quad u_4 \quad u_5 \quad u_6]^T$ can be defined using

$$\begin{pmatrix} u_{1ot} \\ u_2 \\ u_3 \\ u_4 \\ u_5 \\ u_6 \end{pmatrix} = \frac{1}{2}\begin{pmatrix} I & I \\ I & -I \end{pmatrix}cv\begin{pmatrix} P^{-1}R^T & 0 \\ 0 & Q^{-1} \end{pmatrix}\begin{pmatrix} f_{0_1} \\ f_{0_2} \\ f_{0_3} \\ t_{b_1} \\ t_{b_2} \\ t_{b_3} \end{pmatrix}$$

(1) $\quad P = \hat{k}\begin{pmatrix} 0 & 1 & 0 \\ 1 & 0 & 0 \\ 0 & 0 & 1 \end{pmatrix} \qquad Q = \frac{\hat{k}l}{\sqrt{2}}\begin{pmatrix} 1 & 0 & 1 \\ 0 & -1 & 1 \\ 1 & -1 & 0 \end{pmatrix}$

$$S = k_T\begin{pmatrix} 0 & 1 & 0 \\ -1 & 0 & 0 \\ 0 & 0 & -1 \end{pmatrix}$$

Where:

f_O = Force demand vector in earth axes (N)

t_b = Torque demand vector in body axes (Nm)

$\hat{k}$ = Coefficient relating pitch to force (N/rad)

l = Rotor arm length (m)

k_T = Coefficient relating pitch to torque (Nm/rad^2)

R^T = Rotational matrix mapping between body

and earth axes

The required pitch angles for each rotor, θ_i, are calculated by substituting the requirements vector $\begin{bmatrix} u_1 & u_2 & u_3 & u_4 & u_5 & u_6 \end{bmatrix}^T$ into Equation 2. $\begin{bmatrix} \theta_4 & \theta_5 & \theta_6 \end{bmatrix}$ are then substituted in Equation 3 to obtain the complete pitch requirement vector.

$$\begin{pmatrix} \theta_4 \\ \theta_5 \\ \theta_6 \end{pmatrix} = \left[\begin{pmatrix} u_4 \\ u_5 \\ u_6 \end{pmatrix} + \frac{1}{2}Q^{-1}S\begin{pmatrix} (u_1+u_4)^2 \\ (u_2+u_5)^2 \\ (u_3+u_6)^2 \end{pmatrix}\right] \times$$

(2) $\left[I + Q^{-1}S\begin{pmatrix} u_1+u_4 & 0 & 0 \\ 0 & u_2+u_5 & 0 \\ 0 & 0 & u_3+u_6 \end{pmatrix}\right]^{-1}$

(3) $\begin{pmatrix} \theta_1 \\ \theta_2 \\ \theta_3 \end{pmatrix} = \begin{pmatrix} u_1+u_4 \\ u_2+u_5 \\ u_3+u_6 \end{pmatrix} - \begin{pmatrix} \theta_4 \\ \theta_5 \\ \theta_6 \end{pmatrix}$

Manual control of the vehicle by the operator can be implemented by using a standard RC controller to control either f_0 or t_b via appropriate scaling and damping. The uncontrolled vector is simply set to 0 (the force input vector includes a gravitational compensation term).

Both control & mapping functions are significantly more computationally expensive than those of a traditional quadrotor. Implementation of the controllers and mapping function in the ArduPilot controller involves translation of the required algorithms into the Wiring language used by Arduino compatible embedded controllers such as the ArduPilot Mega.

This procedure is somewhat complicated by the lack of native matrix support in Wiring itself. Furthermore, the ATmega 1280 lacks a floating-point unit and therefore floating-point arithmetic must be calculated in software. The gyro and accelerometer sensor filtering already makes heavy use of floating-point calculations, restricting CPU cycles available for other parts of the flight control software. Whilst this is not an issue with the current classical controllers, implementation of more computationally expensive controllers may require the control & mapping algorithms to be ported to utilize fixed-point or even integer arithmetic. This should be possible with little or no loss of control quality and would yield significant performance improvement.

3.3 Hardware in the loop simulation

Implementation of the new EVP system for the hexrotor vehicle requires development of a new flight control system in terms of flight control hardware and software.. For the purposes of initial ground testing a hardware-in-the-loop simulation approach has been adopted. This allows testing of the physical embedded flight controller by generating virtual IMU sensor data and feeding them into the controller under test. The generation of virtual data is done by a Simulink model of the vehicle. The controller response is then determined either by direct measurement of the control response signal or by measuring the physical response of the system in terms of the collective pitch angle and the rotational speed of the rotor blades.
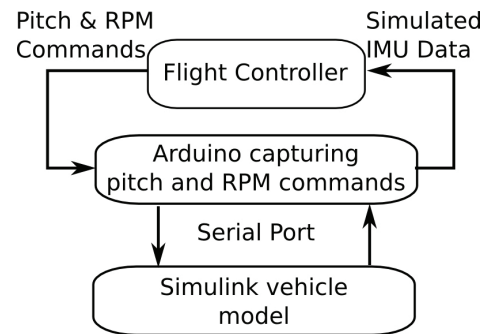

Figure 8: Proposed hardware in the loop setup

Virtual quantities from the simulation model are sent over a serial communication channel to an electrical emulator, which is also based on the Arduino platform. This emulator then transforms the simulated digital data into a proportional analogue voltage signal which is, in turn, fed as input to the flight controller.

This simulation approach allows verification of the basic functionalities of the microcontroller in response to the

simulated environment. This method is suitable for testing operation-critical systems such as flight controllers without the risk of damaging the vehicle. Additional response data (e.g. overall thrust, moments, etc.) will be obtained by placing the integrated vehicle on an appropriate six component force balance.

4   SYSTEM MODELLING

4.1   Modelling concept

A simulation environment for the hexrotor vehicle was created as tool for preliminary design and controller validation. The model is implemented in a modular Simulink system and draws on a range of standalone simulation blocks which could be changed to lower/higher fidelity models as required. The simulation model also includes guidance, visualisation blocks and pilot interface blocks, so that operations can be simulated and visualised up to a mission level.

4.2   Airframe model

The airframe itself is modelled as rigid body with the mass and inertial properties obtained directly from a CAD model. The relatively complex nature of the vehicle geometry means that it is convenient to define both a conventional body axes coordinate frame with x pointing forwards, y to starboard and z down and an additional body fixed frame aligned with the rotor planes as shown in Figure 2. Suitable rotation matrices were employed to resolve earth axes velocities and the local forces on the rotor disks.

Most published work on multi-rotor vehicles, including our previous work [6], treats fuselage aerodynamics as insignificant near hover. To improve the fidelity of the simulation at non hover conditions the airframe aerodynamics are modelled using axial and normal forces as functions of body attitude. The model was calibrated using wind tunnel data from tests on similar-sized multi-rotor fuselage designs at a range of practical body attitudes.

4.3   Rotor aerodynamics modelling

The aerodynamic modelling of the rotors was one of the key modelling challenges since the unconventional arrangement of the rotors lead to rotor disk angle of attack which are not typically found on aircraft propellers or helicopter rotors under normal operating conditions. The simulation had to deliver 6-dof forces/moments and the required rotor power for an initially unknown rotor load and at all velocity vectors of practical interest. Based on these requirements and the need to obtain rapid solutions with modest computing resources, a numerical blade element model was developed. Further details of the model and the wind tunnel validation experiments were published in [13, 14] only a brief summary is presented here.

The inputs to the blade element aerodynamics function are the current velocity vector onto the rotor disk, the rotational speed and the collective pitch angle. Aerofoil chord, pitch and section are treated as functions of the rotor radius and synthetic airfoil data is used to represent the nonlinear lift and drag coefficients at the local blade element Reynolds number for a +/-180 ° angle of attack range. A first order flapping model is used to approximate the tip path plane for a hingeless rotor system.

The induced velocity is approximated by combining a radial inflow variation with a 1st order harmonic inflow model for forward flight [15] or a Mangler & Squire model [16] for advance ratios greater than 0.1. The induced velocity model is used in an iteration loop based on the local velocity vector and loading of every blade element. The iteration loop is stabilised using an over relaxation scheme based on the blade element loading.

The local element loading is resolved into disk forces and moments and fed-back into the vehicle simulation environment. Since the current method is that it does not correctly predict vortex ring state conditions an acceptable vehicle velocity envelope had to be mapped out, so that none of the individual rotors would be subject to vortex ring state conditions. It is also noted that interference effects between rotors are ignored and this assumption is tested experimentally.

4.4   Electric systems modelling

The brushless motor is modelled using a standard 1st order DC motor model, such as presented by Drela [17] and in previous quadrotor design projects [18], and combining it with slight modifications to account for the particular nature of brushless motors. Based on simple parameters from motor datasheets or measurements the electric power consumption, current draw and electric efficiency can be estimated.

A first order model form [18] for lithium-polymer batteries is used with a focus on the battery voltage drop and losses for a given load. It is also used to ensure practical limits on the battery discharge in the simulation model.

4.5   Rotor-motor dynamics

The dynamics of the propulsion system can be roughly broken down into two effects: the rotor aerodynamics and the inertia of the rotor-motor system that is affecting the time constant for changes in rotational speed.

Variable-speed rotor systems can experience a significant delay in the rotational speed response which is largely driven by the inertia of the system [1]. By using a variable-speed design this effect can be avoided, but it is appreciated that further work is required to establish the dynamics of the rpm governor control loops.

For variable-pitch rotors there is a time delay between a pitch actuation and the corresponding thrust change. This delay can be modelled using the time constant of the dynamic inflow ODE [16]

$$(4)\quad \tau_\lambda = \frac{0.849}{4\overline{\lambda_i}\Omega}$$

For a typical hexrotor hover rpm of 8000 ($\Omega = 420$ rad/s), and a mean hover inflow ratio ($\overline{\lambda_i} = 0.086$) this yields a time constant of 3 ms. This delay is 1-2 orders of magnitude small than on full sized helicopters and was considered insignificant for the purpose of this study.

4.6   Experimental validation

Experiments were carried out to evaluate the rotor performance and establish the magnitude of rotor interference effects.
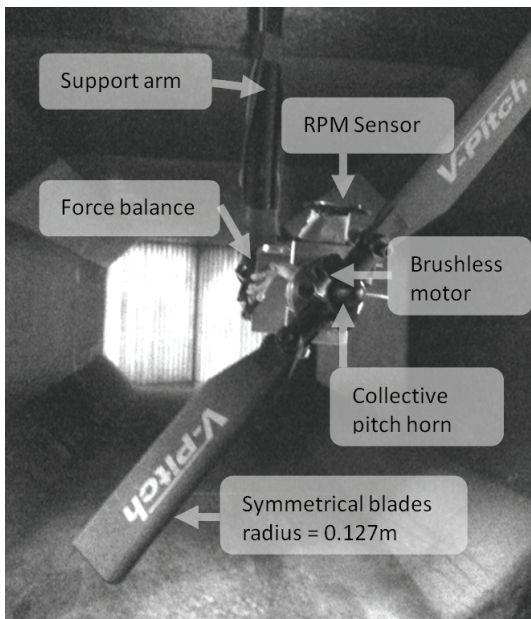
Figure 9: Variable pitch wind tunnel test rig with force balance and rpm sensor. Rotor diameter = 254 mm

The rotor performance was measured on a static testrig and in windtunnel tests a rotor similar to the rotors used on the final design. The test rotors had a radius of 0.127 m, a solidity of 0.099 and symmetrical, untwisted with a constant chord between 40-100% radius. The rotor was tested in an open-circuit blow down low speed tunnel with a 0.9x11.m test section and a turbulence level of 0.5%. A 6-axis force balance was fitted between the motor and the support arm and an overhead yaw control mechanism was used to allow for a 360° rotation. The assembly was equipped with a Hall effect sensor for the rotational speed and pressure transducers for the tunnel velocity.

Real-time data acquisition equipment was used to set demands for collective pitch and rpm and for taking simultaneous measurements of all sensors. The data was post-processed and expressed in nondimensional force coefficient and advance ratios which could be used to partly validate the blade element method over the range of flow conditions of practical interest. Further details of the testing and experiments can be found in [13, 14].

The rotor-rotor interference of the proposed hexrotor rotor arrangement was studied using a geometrically similar fixed-pitch hexrotor mounted on a 6-component force balance. Forces and moments were demanded through the static mapping relationships described in 3.2 and the linearity and off-axes response was studied. In hover interference was found to have negligible effects on net forces and moments [6], although no judgement can be made on interaction effects in forward flight.

5 RESULTS

5.1 Variable pitch operating mode and performance

For an electric variable pitch system the thrust demand can be meet with a range of collective pitch and rotational speed combinations. Using simulations and experimental validation an operating mode was defined to satisfy the key constraint of hovering on two rotors whilst optimising the

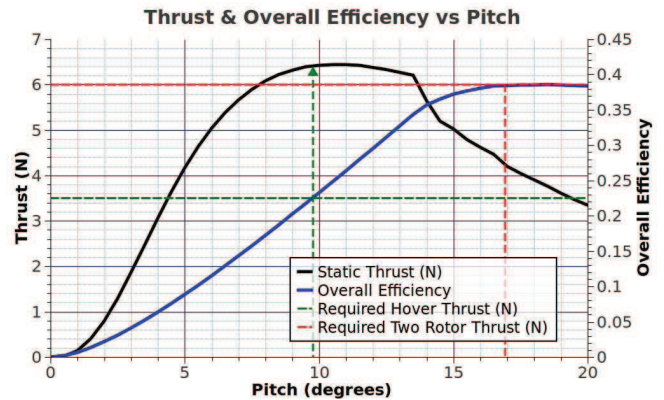combined aerodynamic and motor efficiency for typical hover conditions.

Figure 10: Hover performance validation and efficiency of a single EVP unit

Figure 10 shows single rotor thrust and combined efficiency against collective pitch. It demonstrates the suitability of the proposed EVP system, because the worst case design constraint of lifting the vehicle on two rotors (T=6N) can be satisfied if the system is operated at a sufficiently high base rpm of 12500. This rotational speed also maximises the system efficiency around typical hover conditions (Pitch = 9.5°, T=3.5N) for which the weight support is provided by all six rotors. Around these operating conditions thrust responds linearly to small changes in collective pitch.

The vehicle endurance at the proposed operating conditions was studied as a function of vehicle mass. Based on the availability of suitable batteries and the trade-off between additional battery capacity and increased power demand the maximum endurance for the current design is estimated around 6-7 minutes with a 3.5Ah 3-cell lithium polymer battery. Whilst this endurance is considerable lower than on similarly sized planar rotorcraft vehicles, this is a necessary trade-off resulting from the unique capabilities of the hexrotor design.

5.2 Current state of the project

Based on the method and experiments presented in this paper a prototype of the vehicle has been designed using commercially available parts and open-source electronics solutions. The flight capable version of the prototype, as of August 2011, can be seen in Figure 11.
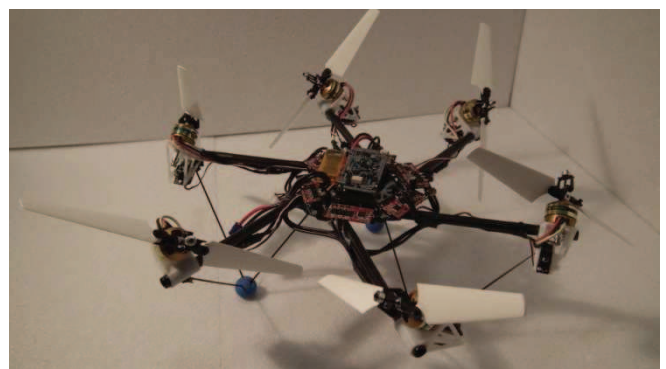

Figure 11: Flight-capable prototype of the variable-pitch hexrotor with assembled EVP units and an Ardupilot mega

Further static and free flight testing of the hexrotor is planned for September 2011.

The take off mass of the prototype is 1.2kg. The mass breakdown in Figure 12 is quite different from traditional coplanar vehicles due to the high propulsion group and low airframe mass fraction.
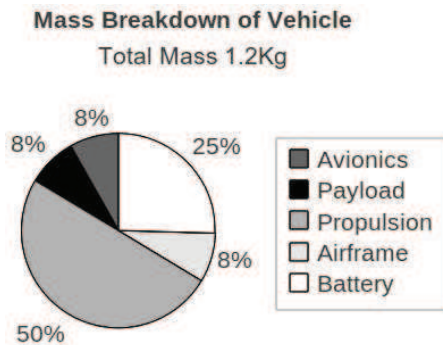

Figure 12: Vehicle mass breakdown

6   CONCLUSIONS

The engineering design for a novel hexrotor vehicle with variable-pitch rotors has been introduced which has the ability to point the thrust vector independent of the body attitude. The key contribution of this paper is to present an engineering and simulation approach that enables the design of such a vehicle with commercially available components and largely open source based software solutions.

It is shown that the key design constraint that arises from the hexrotor concept is the need to provide sufficient thrust with two rotors to lift the entire vehicle, so that thrust can be vectored at any attitude. This requirement has been met by designing an airframe with a mass fraction of around 8% of the all up weight and the selection of an electric variable pitch propulsion system based on a maximum propulsion unit thrust to weight ratio rather than efficiency.

Simulation and testing strategies for the unique rotor arrangement were presented and the feasibility of the propulsion unit static thrust response was demonstrated through ground testing and simulation.

REFERENCES

1.   Pounds, P., Mahony, R., Corke, P.I., *Design of a Static Thruster for Microair Vehicle Rotorcraft.* Journal of Aerospace Engineering, 2009. **22**(1): p. 85-94.

2.   Bouabdallah, S., P. Murrieri, and R. Siegwart, *Towards autonomous indoor micro VTOL.* Autonomous Robots, 2005. **18**(2): p. 171-183.

3.   Hoffmann, G.M., Huang, H., Waslander, S.L. ,Tomlin, C.J., *Quadrotor Helicopter Flight Dynamics and Control: Theory and Experiment*, in *AIAA Guidance, Navigation and Control Conference and Exhibit, 20-23 August 2007*. 2007, AIAA: Hilton Head, South Carolina.

4.   Salazar, S., Romero, H., Lozano, R., Castillo P., *Modeling and Real-Time Stabilization of an Aircraft Having Eight Rotors.* Journal of Intelligent and Robotic Systems, 2009. **54**: p. 455-470.

5.   Crowther, W.J., Lanzon, A., Pilmoor, M., Geoghegan, P., *Rotary Wing Vehicle*, U.K. Patent GB2462452A, Editor. 2008: UK.

6.   Crowther, W.J., Lanzon, A., Maya-Gonzalez, M., Langkamp, D., *Kinematic Analysis and Control Design for a Non Planar Multirotor Vehicle* Journal of Guidance, Control, and Dynamics, 2011. **accepted**.

7.   Bouguet, J.-Y., *Camera calibration toolbox for Matlab*. 2001.

8.   Bradski, G., *The OpenCV Library.* Dr. Dobb's Journal of Software Tools, 2000.

9.   Hirzer, M., *Marker Detection for Augmented Reality Applications* in *Austria Seminar Project*. 2008, Inst. for Computer Graphics and Vision Graz University of Technology: Graz.

10.   Anderson, C. *ArduPilot Project*. Available from: http://diydrones.com/profiles/blogs/ardupilot-main-page.

11.   Banzi, M., et al. *Arduino Project*. Available from: http://arduino.cc/.

12.   HiSystems GmbH, *Mikrokopter*. Available from: http://www.mikrokopter.de.

13.   Langkamp, D., Crowther W.J., *A low order rotor aerodynamics model for UAVs in wind*, in *2010 RAeS Aerodynamics Conference - Applied Aerodynamics:Capabilities and Future Requirements*. 2010, RAeS: Bristol.

14.   Langkamp, D., Crowther W.J., *The role of collective pitch in multi rotor UAV aerodynamics*, in *36th European Rotorcraft Forum*. 2010: Paris.

15.   Chen, R.T.N., *A Survey of Nonuniform Inflow Models for Rotorcraft Flight Dynamics and Control Applications*, in *NASA Technical Memorandum 102219*. 1989, Ames Research Centre.

16.   Leishman, J.G., *Principles of Helicopter Aerodynamics 2nd edition*. 2006, Cambridge: Cambridge Aerospace Series.

17.   Drela, M. *Qprop theory document*. 2007; Available from: http://web.mit.edu/drela/Public/web/qprop/.

18.   Stepaniak, M.J., *A Quadrotor Sensor Platform*, in *Russ College of Engineering and Technology*. 2008, Ohio University.